

Angular Dependence of the Spin-Polarization Transfer from Circularly Polarized Synchrotron Radiation onto Photoelectrons from Atomic Xe $5p^6$

Ch. Heckenkamp, F. Schäfers, G. Schönhense, and U. Heinzmann

Fritz-Haber-Institut der Max-Planck-Gesellschaft, D-1000 Berlin 33, West Germany

(Received 28 November 1983)

The photoelectron emission from atomic xenon has been simultaneously resolved with respect to photon energy, photon (circular) polarization, photoelectron emission angle, electron kinetic energy, and spin-polarization components by use of synchrotron radiation of wavelengths between 48 and 90 nm from the new dedicated electron storage ring BESSY. The angular dependence of the spin polarization and the energy dependence of the dynamical spin parameters experimentally obtained show good agreement with theoretical predictions.

PACS numbers: 32.80.Fb

Experimental analysis of photoelectron-spin polarization in photoionization using circularly polarized light (Fano effect¹) was up to now restricted to angle-integrated measurements² without resolution of the kinetic energy of the photoelectrons corresponding to different ionic states. With the development of the electron storage ring BESSY, a light source of circularly polarized vacuum ultraviolet (vuv) radiation with sufficiently high intensity has become available, which makes angle- and energy-resolved spin-polarization transfer studies from circularly polarized radiation onto photoelectrons feasible.

It is the purpose of this Letter to report on the first experiment in which all four dynamical parameters describing the angular dependences of the three components of the electron-spin polarization vector have been determined simultaneously. We focus, however, on the polarization component (parallel to the photon momentum) which is proportional to the degree of circular polarization of the vuv radiation absorbed (spin-polarization transfer), because the component perpendicular to the photoionization reaction plane (defined by the directions of incoming light and outgoing photoelectron) also appears if unpolarized or linearly polarized radiation is used, as previously studied³ with resonance line radiation.

For elliptically polarized light, the photoelectron-spin polarization not only depends on the polar emission angle θ but also on the azimuthal orientation φ . For $\varphi = 45^\circ$ of the reaction plane with respect to the principal axes of the light-polarization ellipse, the spin-polarization component $A_{e11}(\theta)$ parallel to the photon momentum is

given by the relation

$$A_{e11}(\theta) = P_{\text{circ}} \frac{A - \alpha P_2(\cos\theta)}{1 - \frac{1}{2}\beta P_2(\cos\theta)} + P_{\text{lin}} \frac{2\xi \sin^2\theta}{1 - \frac{1}{2}\beta P_2(\cos\theta)} \quad (1)$$

which has been derived from the general relations given by Huang.⁴ $A_{e11}(\theta)$ is characterized by the four dynamical parameters⁵ A , α , ξ , and β , where A is the angle-integrated spin polarization transfer, α is the asymmetry parameter of the angular-dependent spin-polarization transfer, ξ is the spin parameter describing the spin polarization in ionization using linearly or unpolarized light, and β is the asymmetry parameter of the differential photoionization cross section. The first term in Eq. (1) changes its sign when left-handed instead of right-handed elliptically polarized light is used, whereas the second term does not, because it is only due to the admixture of linear polarization in the elliptically polarized light.

In addition to $A_{e11}(\theta)$, an angular-dependent component $P_{\perp}(\theta)$ normal to the reaction plane occurs⁵:

$$P_{\perp}(\theta) = \frac{2\xi \sin\theta \cos\theta}{1 - \frac{1}{2}\beta P_2(\cos\theta)}. \quad (2)$$

This component exists independent of the state and degree of polarization of the ionizing radiation. The third component of the electron-spin polarization vector, perpendicular to the photon momentum but in the reaction plane, contains no independent information.⁴ All four dynamical parameters describing the photoelectron-spin po-

larization can therefore be extracted from the measurements of $A_{\text{e}11}(\theta)$ and $P_{\perp}(\theta)$.⁶

In practice, the spin-polarization transfer $A(\theta)$, which is equal to $A_{\text{e}11}(\theta)$ in the ideal case of complete circular polarization σ^+ , is determined by combination of Eqs. (1) and (2) with use of the measured data of $A_{\text{e}11}(\theta)$, $P_{\perp}(\theta)$, P_{circ} and P_{lin} :

$$A(\theta) = \frac{A - \alpha P_2(\cos\theta)}{1 - \frac{1}{2}\beta P_2(\cos\theta)} = \frac{A_{\text{e}11}(\theta) - P_{\text{lin}} P_{\perp}(\theta) \tan\theta}{P_{\text{circ}}} \quad (3)$$

We briefly discuss the main components of the apparatus, partly shown in Fig. 1. The synchrotron radiation is dispersed by a 6.5-m N. I. monochromator of the Gillieson type,⁷ not shown in Fig. 1, with the electron beam in the storage ring being the virtual entrance slit. A spherical mirror and a plane holographic grating (1200 lines/mm) form a 1:1 image of the tangential point in the exit slit. With a slit width of 2 mm a bandwidth of 0.5 nm has been achieved. Apertures movable in the vertical direction are used to select radiation emitted above or below the storage ring plane, which has positive or negative helicity, respectively.

The monochromatized and elliptically polarized light crosses the atomic beam producing photoelectrons in a region free of electric or magnetic fields. The photoelectrons emitted in the reaction plane at an angle θ are energy analyzed in a simulated hemispherical electron spectrometer,⁸ which is rotatable around the normal of the reaction plane. An electrostatic deflection by 90° di-

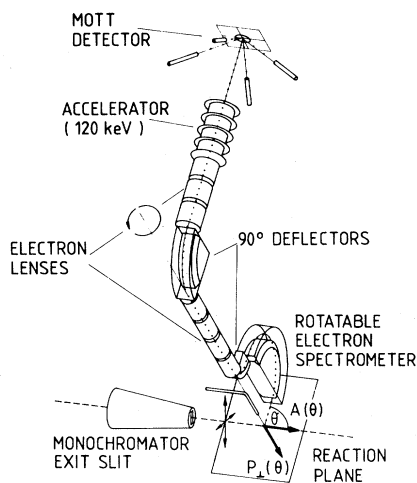


FIG. 1. Schematic diagram of the apparatus.

rects the electron beam along the axis of rotation of the electron spectrometer. After a second deflection by 90° the electron beam is accelerated to 120 keV and scattered at the gold foil of the Mott detector.² $A(\theta)$ and $P_{\perp}(\theta)$, both being transverse components, are simultaneously determined from the left-right scattering asymmetry measured by two pairs of detectors as shown in Fig. 1. Instrumental asymmetries could be easily eliminated by taking advantage of the reversal of the light helicity and of the change of the emission angle from θ to $-\theta$ as well as by use of four additional detectors in forward scattering directions in the Mott detector, not shown in Fig. 1.

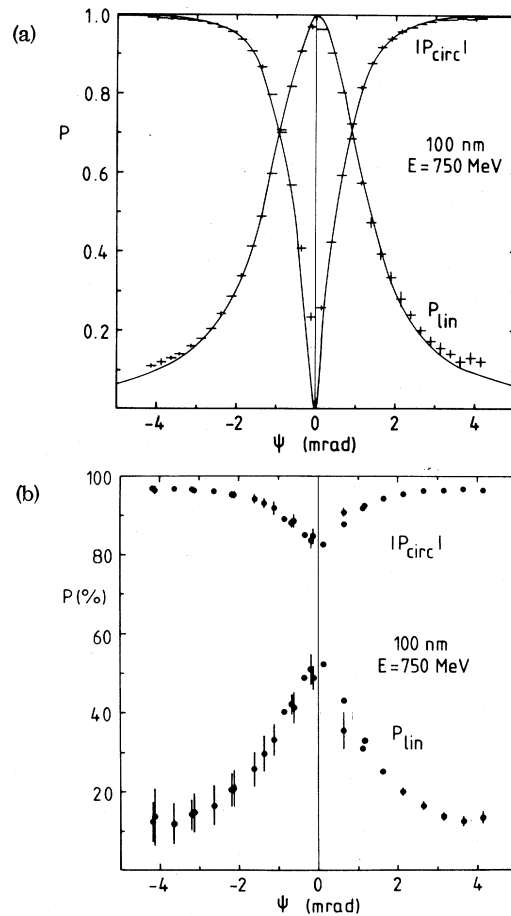


FIG. 2. Degree of circular and linear polarization, P_{circ} and P_{lin} , respectively, of vuv synchrotron radiation emitted from the BESSY storage ring plane (a) as function of the vertical angle ψ (± 0.1 mrad), where the solid lines represent the theoretical prediction according to Schwinger's theory; and (b) in a vertical angular range from ψ to ± 5 mrad. The wavelength dependence of P_{circ} and P_{lin} between 50 and 100 nm is negligible.

P_{circ} and P_{lin} have been measured by means of a rotatable four-mirror analyzer² not shown in Fig. 1. Figure 2 shows the results for P_{circ} and P_{lin} as functions of the vertical angle ψ . The vertical apertures of the monochromator were open during the measurements shown in Fig. 2(a) so that $\Delta\psi = \pm 0.1$ mrad [shown by the horizontal error bars in Fig. 2(a)], whereas in Fig. 2(b) the vertical angular ranges were from ψ to ± 5 mrad. The photoelectron-spin-polarization studies have been performed with $P_{\text{circ}} = \pm 95\%$ and $P_{\text{lin}} = 31\%$ [corresponding to $\psi = \pm 1$ mrad in Fig. 2(b)]. Under these conditions a photon flux on the order of 10^{11} s^{-1} (200 mA beam current) passed the monochromator exit slit and the atomic beam. Typical count rates in the counters in the Mott detector were 0.5 to 8 s^{-1} , one order of magnitude more than the corresponding background.

For the determination of A and ξ from Eqs. (3) and (2), respectively, a spin-polarization measurement at the "magic angle" $\theta_m = 54.7^\circ$, where the second Legendre polynomial $P_2(\cos\theta)$ vanishes, is sufficient. The spin parameter α , however, can only be obtained from measurements at different angles θ . Before relying on the determination of α values from measurements at a few angles only, we felt the necessity to check the validity of the theoretical prediction of the complete angular dependence $A(\theta)$. This has been performed at a wavelength of 80 nm for photoelectrons which correspond to the final ionic

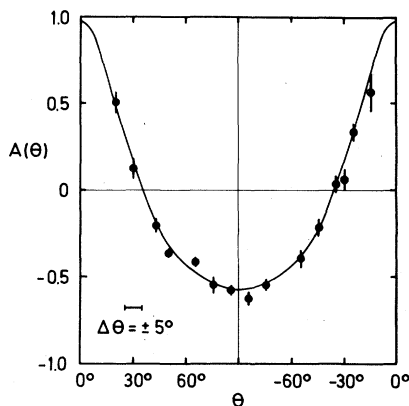


FIG. 3. Angular dependence of the spin-polarization transfer $A(\theta)$ from circularly polarized radiation (80 nm) onto photoelectrons leaving the xenon ion in the $^2P_{1/2}$ state. The least-squares fit (solid curve) yields the dynamical parameters $A = -0.39 \pm 0.01$, $\alpha = -0.74 \pm 0.03$, $\xi = 0.30 \pm 0.03$, $\beta = 1.28 \pm 0.10$. The values for ξ and β agree well with the results of former studies (Refs. 3 and 9) within the error bars.

state $\text{Xe}^+ ^2P_{1/2}$. The results are shown in Fig. 3. The error bars include the single statistical errors of the spin-polarization analysis, the error in the determination of the light polarization, as well as the uncertainty in the analyzing power of the Mott detector. A least-squares fit of $A(\theta)$ to the measured values according to Eq. (3) shows the validity of the theoretical prediction.^{4,5} Furthermore, the fit gives the value $A(0) = 0.97 \pm 0.08$. This means that within the error limits the photoelectrons emitted into the forward direction ($\theta = 0$) have been found to be completely spin polarized, which was explicitly theoretically predicted for $^2P_{1/2}$ final ionic states by Brehm¹⁰ a decade ago.

The experimental results for α and A obtained from $A(\theta)$ measured usually at four different angles θ in the wavelength range between threshold and 48 nm for the two final ionic states $\text{Xe}^+ ^2P_{1/2}$ and $^2P_{3/2}$ are shown in Fig. 4. Theoretical predictions for α and A calculated in relativistic random-phase approximation (RRPA) and in RPA with exchange (RPAE), both taking into account many-electron correlations between the $5p^6$, $5s^2$, and $4d^{10}$ subshells, are also shown in Fig. 4 as the solid¹¹ and dashed¹² curves, respectively. The overall agreement with the experimental data confirms the validity of the theoretical predic-

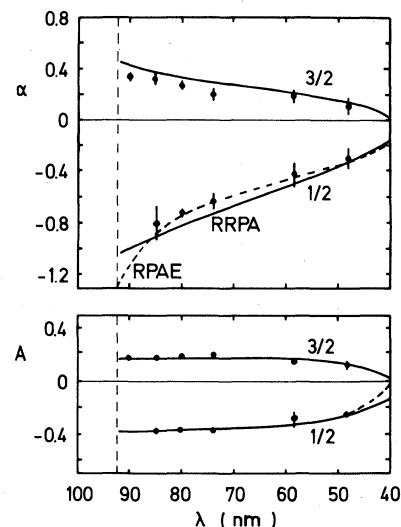


FIG. 4. Experimental results of the spin parameters α and A , upper and lower part, respectively, as functions of the radiation wavelength for photoelectrons leaving the xenon ion in the $^2P_{3/2}$ and $^2P_{1/2}$ final states in comparison with theoretical predictions: RRPA, Ref. 11 (solid curve); and RPAE, Ref. 12 (dashed curve).

tions, although it was surprising that the nonrelativistic RPAE calculation of $\alpha_{1/2}$ is somewhat closer to the measured values than the relativistic theory.

It is worth noting that the quantity $A = A(\theta_m)$ shown in Fig. 4 which has the meaning of an angle-integrated spin-polarization transfer could not be studied in former measurements² of the Fano effect. In these previous experiments, the use of the electric field to collect all photoelectrons produced regardless of their direction of emission forbade the application of an electron spectrometer in order to separate the two fine-structure components, resulting in an average value of $A_{3/2}$ and $A_{1/2}$ close to zero.

In conclusion, the measurements described in this Letter are the last step in the development of a "complete" photoemission experiment¹³: the four parameters of Eqs. (1) and (2), A , α , ξ , and β , together with the absolute photoionization cross section measured by other authors form a complete quantum mechanical characterization of the $5p$ photoionization of xenon atoms. Because of its tuneability, the use of circularly polarized synchrotron radiation overcomes furthermore the disadvantages of previous work using the unpolarized radiation of resonance light sources³. This opens up the possibility to extend the angle- and spin-resolved photoelectron spectroscopy to autoionization resonance regions.¹⁴

We gratefully acknowledge the cooperation of the BESSY staff and support by the Bundesminis-

terium für Forschung und Technologie.

¹U. Fano, Phys. Rev. **178**, 131 (1969).

²U. Heinzmann, F. Schäfers, K. Thimm, A. Wolcke, and J. Kessler, J. Phys. B **12**, L679 (1979); U. Heinzmann, J. Phys. B **13**, 4353 (1980).

³U. Heinzmann, G. Schönhense, and J. Kessler, Phys. Rev. Lett. **42**, 1603 (1979); G. Schönhense, Phys. Rev. Lett. **44**, 640 (1980).

⁴K. N. Huang, Phys. Rev. A **22**, 223 (1980).

⁵V. L. Jacobs, J. Phys. B **5**, 2257 (1972); N. A. Cherepkov, Zh. Eksp. Teor. Fiz. **65**, 933 (1973) [Sov. Phys. JETP **38**, 463 (1974)]; C. M. Lee, Phys. Rev. A **10**, 1598 (1974); K. N. Huang, W. R. Johnson, and K. T. Cheng, Phys. Rev. Lett. **43**, 1658 (1979); H. Klar, J. Phys. B **13**, 3117 (1980).

⁶In principle a measurement of $A_{e11}(\theta)$ would suffice for a determination of the four parameters A , α , ξ , and β . In order to reduce the experimental uncertainties of the parameters and to test the reliability of the apparatus, also independent measurements of $P_{\perp}(\theta)$ were performed.

⁷A. Ebers, Ch. Heckenkamp, F. Schäfers, G. Schönhense, and U. Heinzmann, Nucl. Instrum. Methods **208**, 303 (1983).

⁸K. Jost, J. Phys. E **12**, 1006 (1979).

⁹See, e.g., D. M. P. Holland, A. C. Parr, D. L. Ederer, J. L. Dehmer, and J. B. West, Nucl. Instrum. Methods **195**, 331 (1982), and references therein.

¹⁰B. Brehm, Z. Phys. **242**, 195 (1971).

¹¹K. N. Huang, W. R. Johnson, and K. T. Cheng, At. Data Nucl. Data Tables **26**, 33 (1981).

¹²N. A. Cherepkov, J. Phys. B **12**, 1279 (1979).

¹³J. Kessler, Comments At. Mol. Phys. **10**, 47 (1981).

¹⁴W. R. Johnson, K. T. Cheng, K. N. Huang, and M. LeDourneuf, Phys. Rev. A **22**, 989 (1980).